AIP Advances

A reaction diffusion model of pattern formation in clustering of adatoms on silicon surfaces

Trilochan Bagarti, Anupam Roy, K. Kundu, and B. N. Dev

Citation: AIP Advances **2**, 042101 (2012); doi: 10.1063/1.4757592
View online: http://dx.doi.org/10.1063/1.4757592
View Table of Contents: http://scitation.aip.org/content/aip/journal/adva/2/4?ver=pdfcov
Published by the AIP Publishing

A reaction diffusion model of pattern formation in clustering of adatoms on silicon surfaces

Trilochan Bagarti,[1] Anupam Roy,[2,a] K. Kundu,[1,b] and B. N. Dev[2]
[1]*Institute of Physics, Sachivalaya Marg, Bhubaneswar-751005, India*
[2]*Department of Materials Science, Indian Association for the Cultivation of Science, 2A and 2B Raja S. C. Mullick Road, Jadavpur, Kolkata 700032, India*

(Received 16 August 2012; accepted 20 September 2012; published online 1 October 2012)

We study a reaction diffusion model which describes the formation of patterns on surfaces having defects. Through this model, the primary goal is to study the growth process of Ge on Si surface. We consider a two species reaction diffusion process where the reacting species are assumed to diffuse on the two dimensional surface with first order interconversion reaction occuring at various defect sites which we call reaction centers. Two models of defects, namely a ring defect and a point defect are considered separately. As reaction centers are assumed to be strongly localized in space, the proposed reaction-diffusion model is found to be exactly solvable. We use Green's function method to study the dynamics of reaction diffusion processes. Further we explore this model through Monte Carlo (MC) simulations to study the growth processes in the presence of a large number of defects. The first passage time statistics has been studied numerically. [http://dx.doi.org/10.1063/1.4757592]

I. INTRODUCTION

Growth processes on surfaces at nanoscales can show a countless varieties of patterns. Perfectly ordered geometrical structures, random patterns or both could arise in the growth processes depending on the experimental conditions. Formation of self-organized nanostructures has been extensively studied in the past.[1] Preferential nucleation of the self-organized nanostructures along step edges,[2–4] dislocations[5–8] or domain boundaries[9,10] has been observed. It has been observed that for the Ge adatoms deposited on the Si surface there is a preferential growth at the domain boundaries.[11] Also random clusters are formed at the location of surface defects present inside the domain boundary. These domain boundaries and surface defects act as traps for the deposited adatoms. We present here a reaction diffusion model for these growth processes and pattern formation. This work has been motivated by experimental work on pattern formation in the deposition of Ge on Si(111)-(7 $\times$ 7) surfaces[11] as well as several other previous investigations.[2–10] We note that ours is a case of reaction-diffusion process in random media.

Reaction diffusion processes in random media has been extensively studied in the past. The models that are considered consist of diffusion limited reactions of a single species in the presence of static and moving traps. The traps are the sites where the reactant species get partially or completely adsorbed. These models have been used to explain various processes such as trapping of exciton in a crystal at a defect, electron-hole and soliton-antisoliton recombination, chemical binding of interstitial hydrogen atoms by impurities.[12] Various aspects of reaction-diffusion processes in disordered media such as self-segregation of diffusing particles,[13,14] long time behavior of decay of particle density,[15–17] the kinetics of diffusion limited coalescence and annihilation in random

[a]Also at Microelectronics Research Center, J J Pickle Research Campus, The University of Texas at Austin, Texas 78758, USA.
[b]Corresponding author. Email: kundu@iopb.res.in, Tel: +91-0674-2306406, Fax: +91-0674-2300142.

media,[18–21] have been studied. Recently, the effect of quenched disorder and internal noise on the transport properties in a reaction diffusion model has been studied for 'birth-death' process in a real world situation.[22] Fertile patches called oasis lay randomly in the desert where the population can multiply by birth process and in the desert the population decays due to death processes. Reaction-diffusion in disordered systems is also used to model the decay and preservation of marine organic carbon.[23]

The model that we study here consists of two species linear reaction diffusion processes in the presence of reaction centers (surface defects). Our primary interest is to describe the reaction-diffusion of Ge adatoms on the Si surface. However, this model can be used in cases where the process is occuring on a two dimensional surface. Reactions take place only in a small neighborhood of the defects present on the Si surface. Earlier we had reported some results of a two species reaction diffusion process in the presence of ring defects.[24]

The organization of this paper is as follows. In section II we describe theoretical models. The ring and the point models are discussed. Greens function method is used for the solution of our reaction diffusion equation. In section III we will describe the Monte Carlo simulations and discuss the numerical results for the point defect model. Time evolution of the growth processes is studied from the obtained solutions. We will show that this reaction diffusion model shows the pattern formation that were experimentally reported earlier. Through the MC simulations we investigate the first passage statistics. The first passage time studied here gives us an estimate of the time a particle takes from the origin to reach the domain boundary. This provide us the time scale for the growth process at the domain boundary. The mean first passage time and the first passage time probability density are calculated numerically. The large time assymptotic is discussed in section IV. Finally conclusions are drawn in section V.

II. FORMULATION OF THE MODEL

The model consist of the reaction-diffusion processes of two species S and P on a two dimensional flat surface. Here S denotes the Ge adatoms and P denotes the sum total of possible Ge-clusters. The reaction $S \rightleftharpoons P$ occurs at the location of the defects present on the surface. We call these defects as reaction centers. The reaction scheme is chosen here to describe the clusterization process (see Appendix A). We are considering a sequential clusterization process in this model, however, the actual clusterization process could be quite complicated. The coupled reaction diffusion equations are given by

$$\begin{aligned}\partial_t S(\mathbf{r},t) &= D_s \mathcal{L} S(\mathbf{r},t) - K_f(\mathbf{r}) S(\mathbf{r},t) - K_R(\mathbf{r}) S(\mathbf{r},t) + K_b P(\mathbf{r},t) + J(\mathbf{r},t),\\ \partial_t P(\mathbf{r},t) &= D_p \mathcal{L} P(\mathbf{r},t) - K_b(\mathbf{r}) P(\mathbf{r},t) + K_f(\mathbf{r}) S(\mathbf{r},t),\end{aligned} \tag{1}$$

where $S(\mathbf{r},t)$ and $P(\mathbf{r},t)$ are the concentrations at position $\mathbf{r}$ and time t, D_s and D_p are the diffusion coefficients and $K_f(\mathbf{r})$ and $K_b(\mathbf{r})$ are the reaction rates. The reaction rates are given by $K_\alpha(\mathbf{r}) = k_\alpha \delta(\mathbf{r}-\boldsymbol{\rho})$, for $\boldsymbol{\rho} \in \Omega$. The set Ω denotes the regions on the Si surface where defects are located. The domain boundary is modelled as a ring of radius R and is given by $K_R(\mathbf{r}) = k_R \delta(|\mathbf{r}| - R)/|\mathbf{r}|$. This is no restriction of the proposed model. Any type of boundary can be considered. Then the model will require a fullscale numerical approach. $J(\mathbf{r},t)$ is an external flux. Equation (1) is subject to the boundary conditions $S(\mathbf{r},t)$, $P(\mathbf{r},t)$ are finite at the origin and vanishes at infinity. The initial conditions are $S(\mathbf{r},0) = P(\mathbf{r},0)$=0. Let $\phi(\mathbf{r},s)$, $\psi(\mathbf{r},s)$ and $\hat{J}(\mathbf{r},s)$ be the Laplace transform of $S(\mathbf{r},t)$,$P(\mathbf{r},t)$ and $J(\mathbf{r},t)$ respectively. From Eq. (1) we have

$$\begin{aligned}|\phi(s)\rangle &= G_s^{(1)}(s) D_s^{-1}(-K_f|\phi(s)\rangle + K_b|\psi(s)\rangle + |\hat{J}(s)\rangle),\\ |\psi(s)\rangle &= G_p^{(0)} D_p^{-1}(-K_b|\psi(s)\rangle + K_f|\phi(s)\rangle).\end{aligned} \tag{2}$$

where $\langle \mathbf{r}\,|\,\phi(s)\rangle = \phi(\mathbf{r},s)$, $\langle \mathbf{r}\,|\,\psi(s)\rangle = \psi(\mathbf{r},s)$, $\langle \mathbf{r}\,|\,\hat{J}(s)\rangle = \hat{J}(\mathbf{r},s)$, $\delta(\mathbf{r}-\mathbf{r}')\,K_j(\mathbf{r}) = \langle \mathbf{r}|K_j|\mathbf{r}'\rangle$ for $j = f, b, R$, $\langle \mathbf{r}|(sD_s^{-1} - \mathcal{L})|\phi(s)\rangle = (sD_s^{-1} - \mathcal{L})\phi(\mathbf{r},s)$ and $\langle \mathbf{r}|(sD_p^{-1} - \mathcal{L})|\phi(s)\rangle = (sD_p^{-1} - \mathcal{L})\psi(\mathbf{r},s)$.[25] The orthogonality and the completeness relations are given as $\langle \mathbf{r}|\mathbf{r}'\rangle = \delta(\mathbf{r}-\mathbf{r}')$ and $\int |\mathbf{r}\rangle\langle\mathbf{r}| d\mathbf{r} = 1$.[25] The operator $\mathcal{L}$ is the Laplacian in polar coordinate system.[28]

The Green's function are defined by

$$G_p^{(0)}(s) = [sD_p^{-1} - \mathcal{L}]^{-1},$$
$$G_s^{(0)}(s) = [sD_s^{-1} - \mathcal{L}]^{-1},$$
$$G_s^{(1)}(s) = [sD_s^{-1} - \mathcal{L} + D_s^{-1}K_R]^{-1}. \tag{3}$$

The domain boundary is a circle of radius R so that we can write $K_R = |R\rangle k_R \langle R|$. Expression for $G_s^{(1)}(s)$ can be written in terms of the t-matrix as

$$G_s^{(1)}(s) = G_s^{(0)}(s) + G_s^{(0)}(s)T_R(s)G_s^{(0)}(s) \tag{4}$$

where the t-matrix $T_R(s)$[25] is given by

$$T_R(s) = -(D_s^{-1}K_R - D_s^{-1}K_R G_s^0(s)D_s^{-1}K_R + D_s^{-1}K_R G_s^0(s)D_s^{-1}K_R G_s^0(s)D_s^{-1}K_R \ldots)$$
$$= \frac{|R\rangle(-k_R/D_s)\langle R|}{1 + (k_R/D_s)\int G_s^{(0)}(R,\theta|R,\theta)d\theta} \tag{5}$$

The Green's function in the limit $k_R \to \infty$ is

$$G_s^{(1)}(s) = G_s^{(0)}(s) - \frac{G_s^{(0)}(s)|R\rangle\langle R|G_s^{(0)}(s)}{\int G_s^{(0)}(R,\theta|R,\theta)d\theta} \tag{6}$$

The expressions for $G_\alpha^{(0)}(s)$ and $G_\alpha^{(1)}(s)$ are given in Appendix B. Equation (4) and (5) can also be written in terms of Feynman diagrams (see Fig. 10). Using these expression in Eq. (2), $|\phi(s)\rangle$ and $|\psi(s)\rangle$ can be written in terms of the Green's functions. The concentraions can then be calculated by inverse Laplace transformation of $|\phi(s)\rangle$ and $|\psi(s)\rangle$. At the domain boundary the reaction $S \to S'$ takes place at a rate k_R which is suffifiently high. This implies that those particles that reaches the domain boundary get permanently trapped there.

A. The ring model

The reaction centers are modelled as concentric rings with center at the origin. Due to the circular symmetry we have $\mathcal{L} = \frac{1}{r}\frac{d}{dr}\left(r\frac{d}{dr}\right)$. The concentrations are given by $S(r, t)$ and $P(r, t)$. The reaction rates are given by $K_\alpha(r) = k_\alpha \sum_{r_i} \delta(r - r_i)/r$, where index α is f or b and r_i denotes the collection of all random variable uniformly distributed in $(0, R)$. Thus Ω is defined by the collection of all these circles. A particle flux $J(\mathbf{r}, t)$ is incident normal to the surface. We asume $J(\mathbf{r}, t) = j_0 exp(-\lambda r)$ to be exponentially decaying. Here the reaction $S \rightleftharpoons P$ occurs at the i-th ring and there is diffusion away from the ring. At the boundary $r = R$ the reaction $S \to S'$ takes place at a rate k_R. The diffusion constant of S' is assumed very low as compared to that of S and P. Let $\phi(r, s)$, $\psi(r, s)$ and $\hat{J}(r, s) = j_0 exp(-\lambda r)/s$ be the Laplace transform of the concentrations $S(r, t)$, $P(r, t)$ and $J(r, t)$ respectively. We obtain $\phi(r, s)$ and $\psi(r, s)$ in terms of the Green's function $G_s^{(1)}(r|r')$ and $G_p^{(0)}(r|r')$.

$$\phi(r, s) = \sum_{\{r_i\}} G_s^{(1)}(r|r_i)\rho_1(r_i, s) + Q(r, s),$$
$$\psi(r, s) = \sum_{\{r_i\}} G_p^{(0)}(r|r_i)\rho_2(r_i, s),$$
$$\rho_1(r_i, s) = \frac{k_b}{D_s}\psi(r_i, s) - \frac{k_f}{D_s}\phi(r_i, s),$$
$$\rho_2(r_i, s) = \frac{k_f}{D_p}\phi(r_i, s) - \frac{k_b}{D_p}\psi(r_i, s). \tag{7}$$

where $Q(r, s) = (2\pi/D_s)\int G_s^{(1)}(r|r')\hat{J}(r', s)r'dr'$. Using Eqs. (3) the Green's function can be written as

$$G_\alpha^{(0)}(r|r') = \frac{1}{2\pi} I_0(\sqrt{s/D_\alpha}r)K_0(\sqrt{s/D_\alpha}r'), \tag{8}$$

where the index α is s or p and $r < r'$. When $r > r'$ replace r by r' and vice versa in Eq. (8). In $G_\alpha^{(0)}(r|r')$ the Laplace variable s has been kept implicit for clarity. It will be explicitly written as $G_\alpha^{(0)}(r, r', s)$ whenever required. The presence of the domain boundary $K_R(r)$ acts as a defect. So, we can write the Green's function in the presence of single defect as

$$G_s^{(1)}(r|r') = G_s^{(0)}(r|r') - \frac{G_s^{(0)}(r|R)G_s^{(0)}(R|r')}{G_s^{(0)}(R|R)}. \tag{9}$$

in the $\lim k_R \to \infty$, which makes the domain boundary a perfect sink at $r = R$. Now, suppose there are N_D number of defects. Setting $r = r_j$ for all $j = 1, 2, \ldots, N_D$ in Eq. (2) we obtain $2N_D$ linear equations which can be solved to obtain $\phi(r_j, s)$ and $\psi(r_j, s)$ for all $j = 1, 2, \ldots, N_D$. From Eq. (7) $S(r, t)$ and $P(r, t)$ can then be obtained using Inverse Laplace transform. Let us now consider the case of a single defect. From Eq. (7) we have

$$\phi(r, s) = Q(r, s) - \frac{k_f}{D_s}\frac{G_s^{(1)}(r|r_1)Q(r_1, s)}{\Delta(r_1)}, \tag{10}$$

$$\psi(r, s) = \frac{k_f}{D_p}\frac{G_p^{(0)}(r|r_1)Q(r_1, s)}{\Delta(r_1)}, \tag{11}$$

where $\Delta(r_1) = 1 + (k_f/D_s)G_s^{(1)}(r_1|r_1) + (k_b/D_p)G_p^{(0)}(r_1|r_1)$. We notice from Eq. (10) that, the inverse Laplace transform of the first part $Q(r, s)$ gives the solution of the diffusion equation with a sink at $r = R$ in the presence of external flux. The second part involves a convolution in time the effect of which is to decrease the concentration near the reaction center. Similarly from Eq. (11) we can see the converse. For large number of defects $\phi(r, s)$ and $\psi(r, s)$ will be too complicated, but the concentrations will show the same behavior close to the defect centers. We have implemented the Talbot Inverse Laplace transformation method[27] in our numerical computations. In Fig. 2 we use the domain boundary as the unit circle so that $0 \le r \le 1 (= R)$. In Fig. 2 we plot the concentrations $S(r, t)$ and $P(r, t)$ at time $t = 1.0$ for $D_s = 0.1$, $D_p = 0.01$, $k_f = k_p = 0.1$. There are four ring defects with radius randomly chosen in (0, 1). The concentaration for P shows peaks of decreasing heights at those radii. This happens due to the exponentially decaying incident flux. We will discuss next in the point model how point defect gives rise to similar peaks. We will see that both models differs only in their geometrical aspects.

B. The point model

In this model, we consider point reaction centers spread uniformly over the surface. Let $\mathbf{r}_i$ be the position of the i-th reaction center where $1 \le i \le N_D$ and N_D is the total number of reaction centers (see Fig. 1(b)). So we have $\Omega = \{\mathbf{r}_1, \ldots, \mathbf{r}_{N_D}\}$ the set of position vectors of reaction centers. The reaction rates are given by $K_\alpha(\mathbf{r}) = k_\alpha \sum_{i=1}^{n} \delta(\mathbf{r} - \mathbf{r}_i)$, where $\alpha = f, b$. The Laplace transform of the concentrations $S(\mathbf{r}, t)$, $P(\mathbf{r}, t)$ are given by

$$\begin{aligned}
\phi(r, \theta) &= \sum_{(r_i, \theta_i)\in\Omega} G_s^{(1)}(r, \theta|r_i, \theta_i)\rho_1(r_i, \theta_i) + Q(r, \theta),\\
\psi(r, \theta) &= \sum_{(r_i, \theta_i)\in\Omega} G_p^{(0)}(r, \theta|r_i, \theta_i)\rho_2(r_i, \theta_i),\\
Q(r, \theta) &= \frac{1}{sD_s}\int G_s^{(1)}(r, \theta|r', \theta')J(r', \theta')r'dr'd\theta',\\
\rho_1(r_i, \theta_i) &= \frac{-k_f}{D_s}\phi(r_i, \theta_i) + \frac{k_b}{D_s}\psi(r_i, \theta_i),\\
\rho_2(r_i, \theta_i) &= \frac{-k_b}{D_p}\psi(r_i, \theta_i) + \frac{k_f}{D_p}\phi(r_i, \theta_i),
\end{aligned} \tag{12}$$

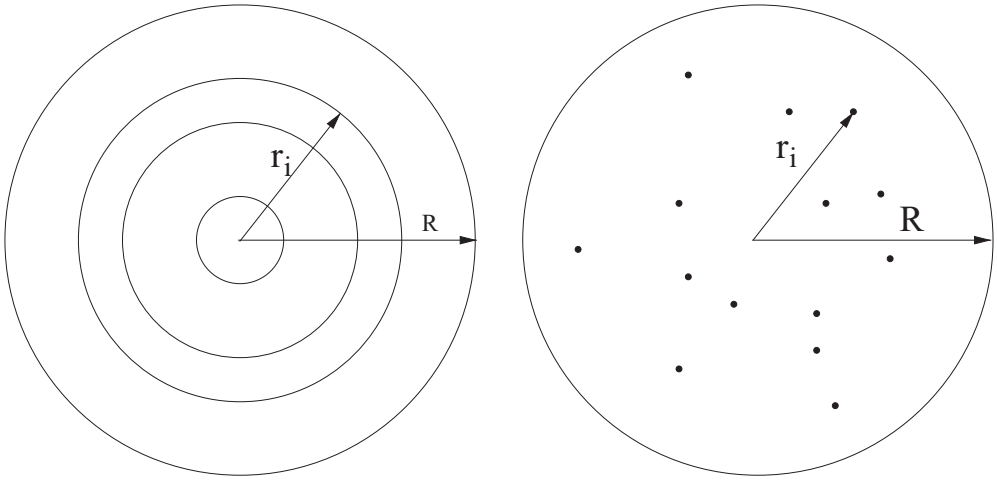

FIG. 1. Geometry of the reaction diffusion process (a) the ring model: the largest ring of radius R denotes the domain boundary, other rings denote the ring defects, (b) the point model: the dots dispersed within the radius *R* denote the point defects on the surface.

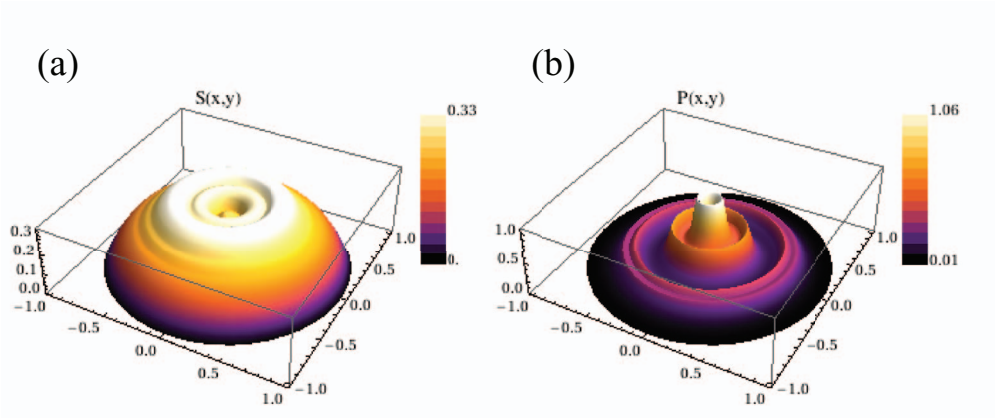

FIG. 2. Concentrations (a) $S(\mathbf{r}, t)$ and (b) $P(\mathbf{r}, t)$ at time $t = 1.0$ where $\mathbf{r} = (x, y)$, $D_s = 0.1$, $D_p = 0.01$, $k_f = 1.0$, $k_p = 0.1$ in the presence of four ring defects in $0 \leq r \leq 1$. Incident flux in exponentially decaying with $\lambda = 1.0$.

Here we have $\mathbf{r} = (r, \theta)$ and $\mathbf{r}_i = (r_i, \theta_i)$ as we are using polar coordinate system. The values of $\phi(r_i, \theta_i)$ and $\psi(r_i, \theta_i)$ can be obtained by solving the following linear equations

$$\phi_i = \sum_{j=1}^{N_D} (G_s^{(1)})_{i,j}(-k_f\phi_j + k_b\psi_j)/D_s + Q_i,$$

$$\psi_i = \sum_{j=1}^{N_D} (G_p^{(0)})_{i,j}(-k_b\psi_j + k_f\phi_j)/D_p. \tag{13}$$

where $(G_s^{(1)})_{i,j} = G_s^{(1)}(r_i, \theta_i|r_j, \theta_j)$, $\phi_j = \phi(r_j, \theta_j)$, $\psi_j = \psi(r_j, \theta_j)$ and $Q_i = 1/(sD_s) \int G_s^{(1)}(r_i, \theta_i|r', \theta')J(r', \theta')r'dr'd\theta'$ for all $i = 1, 2, \ldots, N_D$. Inverting the Eq. (12) and (13) to the time domain will give us the concentrations $S(\mathbf{r}, t)$ and $P(\mathbf{r}, t)$.

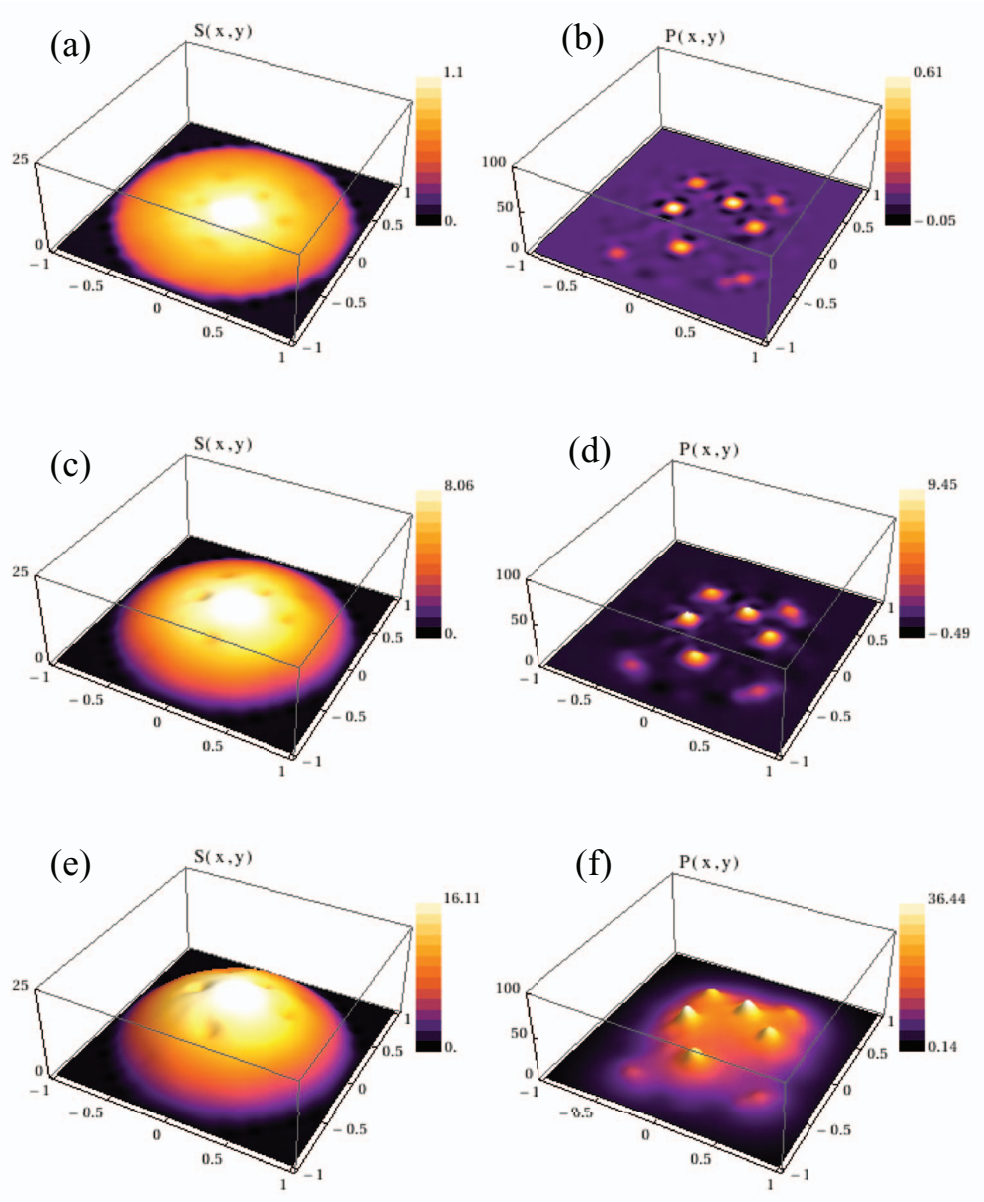

FIG. 3. Concentration $S(\mathbf{r}, t)$ at time (a) $t = 0.01$, (c) $t = 0.1$, (e) $t = 1.0$ and concentration $P(\mathbf{r}, t)$ at time (b) $t = 0.01$, (d) $t = 0.1$, (f) $t = 1.0$ for $D_s = 1.0$ and $D_p = 0.1$.

III. SIMULATIONS AND NUMERICAL RESULTS

We saw earlier that the solution $S(\mathbf{r}, t)$, $P(\mathbf{r}, t)$ can be calculated by using the Green's functions. However for a large number of defects it becomes difficult to evaluate it numerically. We explore numerically the results we have obtained in Eq. (12) for a small number of defect $N_D = 8$. In our computations we have implimented the fixed Talbot method for inverse Laplace transformations.[27] For large number of defects we have studied the system by Monte Carlo simulations. For our numerical computations we have scaled all relevant parameters of the model by the radius of the domain boundary R i.e. $D_\alpha \to \tau D_\alpha/R^2$, $k_\alpha \to \tau k_\alpha$ where the index α is s or p, $\tau = R^2/D_s$ is the unit of time. The values of plots are obtained by setting flux $\tau j_0 \to 1$. The parameter λ is taken as $1/R$ with the assumption that the flux of particles falls off appreciably outside the domain boundary. In the plots in Fig. 3 we show the time evolution of the diffusion process. The following parameters, $D_s = 1.0$, $D_p = 0.1$, $k_f = 0.1$ and $k_b = 0.01$ were used. At $t = 0.01$ (Fig. 3(a) and 3(b)) one can find

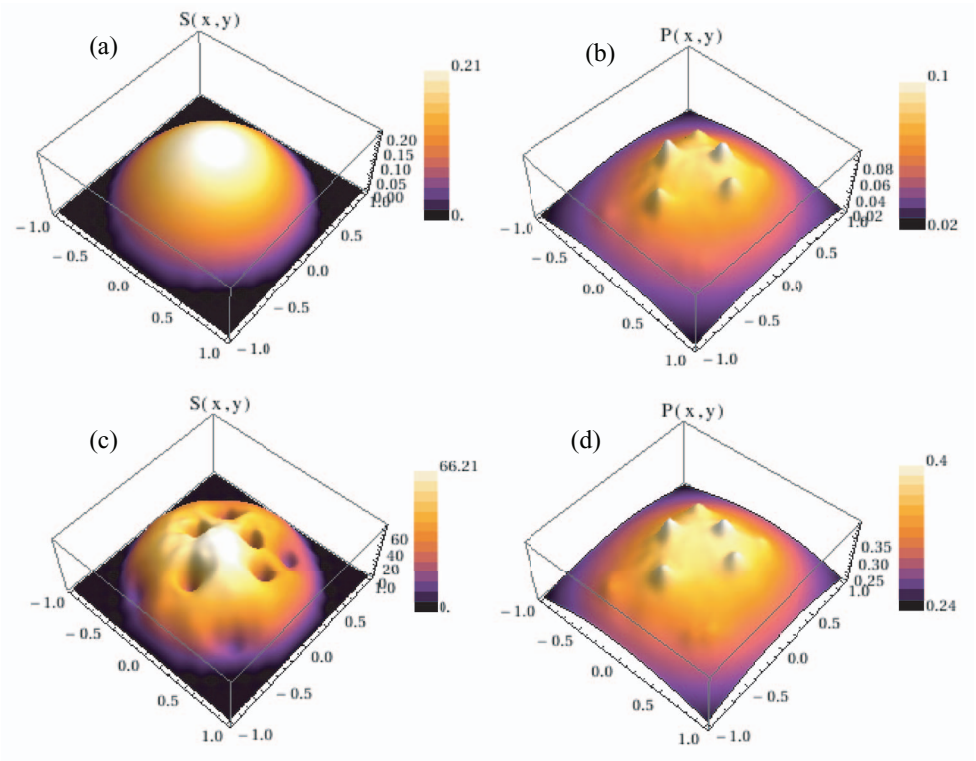

FIG. 4. Concentrations $S(\mathbf{r}, t)$ and $P(\mathbf{r}, t)$: (a,b) for $D_s \gg D_p$ at $t = 1.0$, (c,d) for $D_s \ll D_p$ at $t = 1.0$.

that the reaction has just begun and thus the concentartions of P around the reaction centers can be seen. As we advance ahead in time the concentration of P becomes more prominent and the space between the reaction centers starts filling up due to the diffusion of P. Concentration of S show dips at the locations where the concentration of P peaks. We further note that peaks of P appearing nearer to the origin are higher than those closer to the periphery. This happens as we have chosen an exponentially decaying flux. Asymptotic results were obtained for the following set of parameters $D_s \gg D_p$ with $k_f = k_b = 0.1$ and time $t = 1.0$. Figure 4(a) and 4(b) shows the case for $D_s \gg D_p$. In this case the S species diffuses very fast compared to the P species. Consequently the concentration plot of S shows the expected smoothness. For the opposite case (i.e., $D_s \ll D_p$) we note that (Fig. 4(c) and 4(d)) there are deep hole-like structures in S concentration plot. This means that more number of particles have undergone reactions near the reaction centers as this should be the case for $D_s \ll D_p$. Similarly, if we vary the reaction rate constants we find that the peaks of P grow and dips appear in S with increasing k_f, the rate constant for the conversion of S to P. The concentrations of S and P for $t = 1.0$, $(k_f, k_b) = (0.1, 0.1)$, $(0.5, 0.1)$, $(0.1, 0.5)$ and $D_s = D_p = 1.0$ are plotted in Fig. 5.

For a large number of reaction centers we performed Monte Carlo simulations to study the reaction diffusion process. We have used the stochastic simulation algorithm.[29] Reaction centers are uniformly distributed inside the circular domain of radius R. Each reaction center is a circular disk of radius $a \ll R$ centered at $\mathbf{r}_i$, $i = 1, 2, \ldots N_D$ where the reaction $S \rightleftharpoons P$ take place with rate k_α, $\alpha = f, b$. Outside the circular region there is no reaction. Note that in this numerical approach we allow a definite area for the reaction center. The species S and P freely diffuse with diffusion constant D_s and D_p respectively. Whenever a particle of type S reaches the domain boundary $|\mathbf{r}| = R$ the reaction $S \rightarrow S_1$ occur with probability 1. This makes it a perfect sink (i.e. limit $k_R \rightarrow \infty$). We have taken a constant flux rate J. A snapshot of the simulation with $N_D = 150$ is shown in Fig. 6. The following parameters were used $D_s = 1.0$, $D_p = 0.01$, $D_{S_1} = 0.001$, $k_f = 1.0$, $k_b = 0.1$. The plot shows the density of particles at 5×10^4 Monte Carlo steps. One MC step consist of one diffusive step of each particle on the surface followed by the corresponding reaction step which occurs at rate k_f or k_b depending on the type of particle.

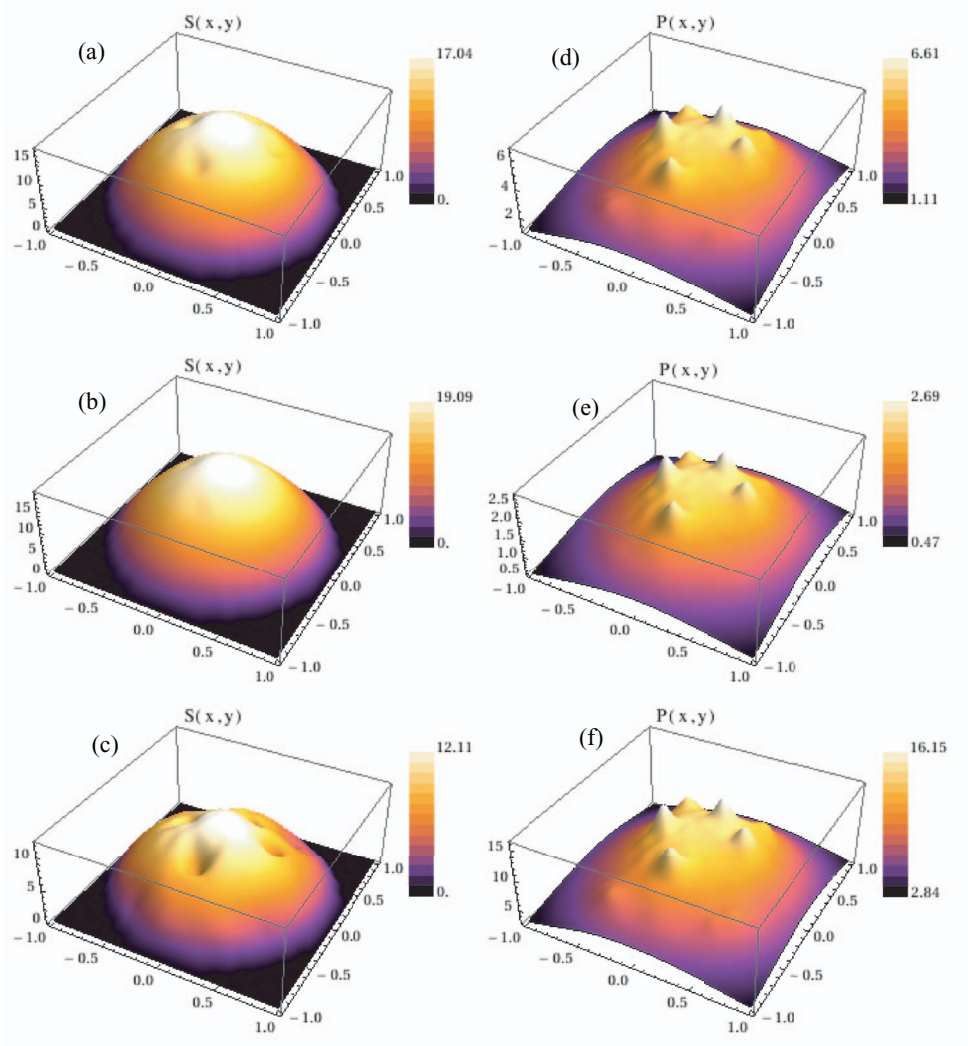

FIG. 5. Concentrations of $S(\mathbf{r})$ (a, b, c) and $P(\mathbf{r})$ (d, e, f): (a, d) $k_f = 0.1$, $k_b = 0.1$, $t = 1.0$; (b, e) $k_f = 0.1$, $k_b = 0.5$, $t = 1.0$; (c, f) $k_f = 0.5$, $k_b = 0.1$, $t = 1.0$.

We have further studied the first passage time statistics of the reaction diffusion process. Starting from the origin at time $t = 0$ a particle of type S undergoes reactions along its path. The diffusion coefficient at a time t depends on whether it is of type S or P. The first passage time is defined as the time required for the particle to reach the domain boundary at R irrespective of its type when it reaches the domain boundary. From our MC simulations we have found that for a fixed N_D the mean first passage time is correlated to the number of reactions the particle undergoes during the entire path. We calculated the mean first passage time and the mean number of reactions as a function of k_b for different values of D_p. The mean first passage time $\langle \tau_f \rangle$ is found to be a strictly decreasing function of k_b. We found that $\langle \tau_f \rangle \sim c_1/(k_b + c_2)$ where c_1 and c_2 are positive constants that depends on D_p. To the best of our knowledge it is a new result.

Let us assume that the probability density of first passage time $P(\tau_f) = p(\tau_f)\exp(-A\tau_f)$ where $p(\tau_f)$ is a positive polynomial and $A > 0$ is a constant. For small values of D_p we have $\langle \tau_f \rangle \sim c_1/k_b$ (see Fig. 7(a) for $D_p < 0.5$). We can assume $p(\tau_f)$ linear which leads to $P(\tau_f) = A^2\tau_f\exp(-A\tau_f)$ where A depends on D_p. This probability density agrees quite well with the results obtained from the MC simulations. The mean first passage time then gives $A = 2k_b/c_1$. In Fig. 8 we plotted the probability density $P(\tau_f)$ for $D_p = 0.1$ and $k_b = 0.1, 0.25, 0.5$ along with the densities obtained from

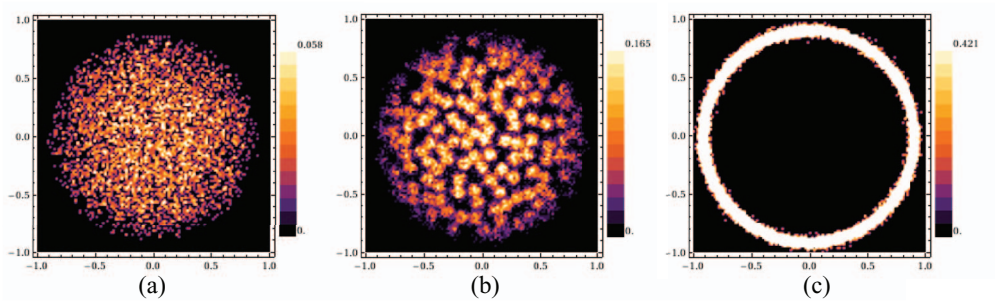

FIG. 6. Snapshots of concentrations: (a) S, (b) P and (c) S_1 obtained from MC simulaion after 5×10^4 MC steps.

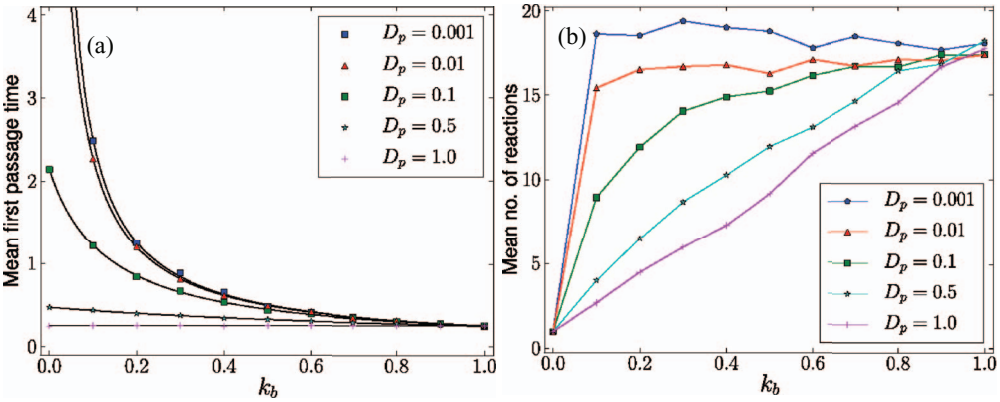

FIG. 7. (a) Mean first passage time and (b) mean number of reaction as a function of k_b. Black lines in (a) is $P(\tau_f)$ that are fit to the MC results(points).$D_s = 1$, $k_f = 1$.

the MC simulations. For small values of D_p we found that the function $P(\tau_f)$ fit very well with the MC results.

IV. ASYMPTOTIC LARGE TIME LIMIT

Consider the ring model with one ring defect. The Green's function in Eq. (10) and (11) when expanded in Taylor series near $s = 0$ can be written as

$$G_s^{(1)}(r|r') \simeq -\frac{1}{2\pi}\left(1+\frac{sr^2}{4D_s}\right)\left(1+\frac{sr'^2}{4D_s}\right)\ln(r'/R)+\ldots,$$

$$G_p^{(0)}(r|r') \simeq \quad -\frac{1}{2\pi}\left(1+\frac{sr^2}{4D_s}\right)\left(1+\frac{sr'^2}{4D_s}\right)\left(\ln\frac{s^{1/2}r'}{2D_s^{1/2}}+\gamma\right)+\ldots,$$

where $r < r'$. For $r > r'$ replace r by r' and vice versa. For $k_f/D_s \ll 1$ and $k_b/D_p \ll 1$ denominator can be approximated as unity. Using the above expressions we have $Q(r, s) \sim s^{-1}$ so that $Q(r, t)$ in the long time asymptotic limit becomes

$$Q^*(r) \simeq \frac{-j_0}{D_s\lambda^2}\{Ei(-\lambda R) - Ei(-\lambda r) + e^{-\lambda r} - e^{\lambda R} + \ln(r/R)\} \tag{14}$$

The concentration $S(r, t)$ and $P(r, t)$ in the asymptotic limit $t \to \infty$[26] can be written as

$$S(r) \simeq Q^*(r) + \frac{k_f}{2\pi D_s}Q^*(r_1)F_1(r),$$

$$P(r) \simeq \frac{-k_b}{2\pi D_p}Q^*(r_1)F_2(r), \tag{15}$$

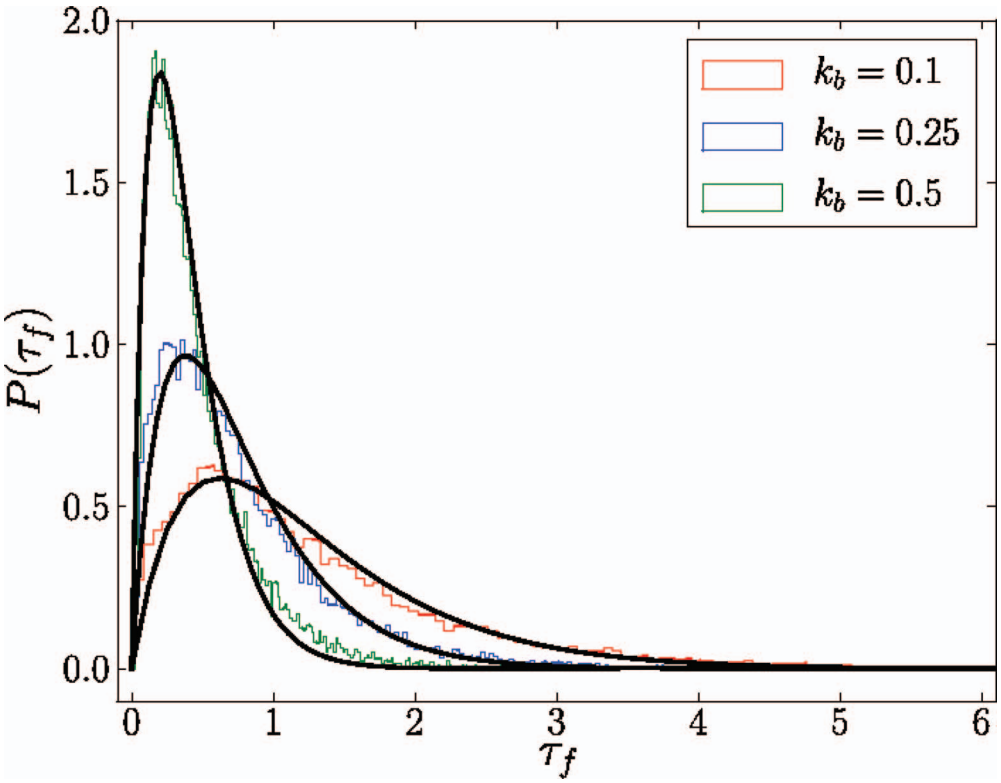

FIG. 8. Comparison of probability densities obtained from MC simulations(thin colored lines) with $P(\tau_f)$ (thick solid lines). $D_s = 1$, $D_p = 0.1$, $k_f = 1.0$.

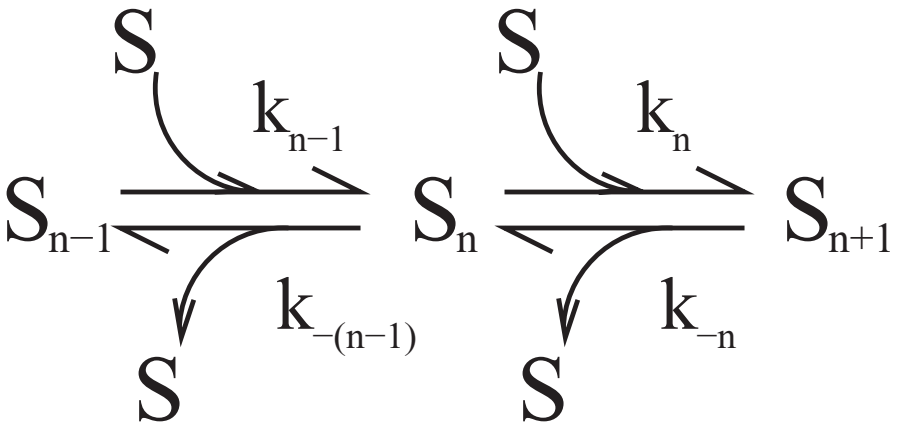

FIG. 9. Reaction scheme.

where

$$F_1(r) = \begin{cases} \ln \frac{r_1}{R} & \text{if} \quad r \le r_1, \\ \ln \frac{r}{R} & \text{if} \quad r > r_1. \end{cases}$$

$$F_2(r) = \begin{cases} \gamma - \frac{1}{2} \ln \frac{4D_p C t}{r_1^2} - \frac{r}{8D_p t} & \text{if} \quad r \le r_1, \\ \gamma - \frac{1}{2} \ln \frac{4D_p C t}{r^2} - \frac{r_1}{8D_p t} & \text{if} \quad r > r_1. \end{cases} \tag{16}$$

and $\gamma = \ln C = 0.5772\ldots$. The function $Q^*(r)$ is a monotonically decreasing function with maximum at the origin $r \to 0$ and zero at the domain boundary $r = R$. From the expression obtained in

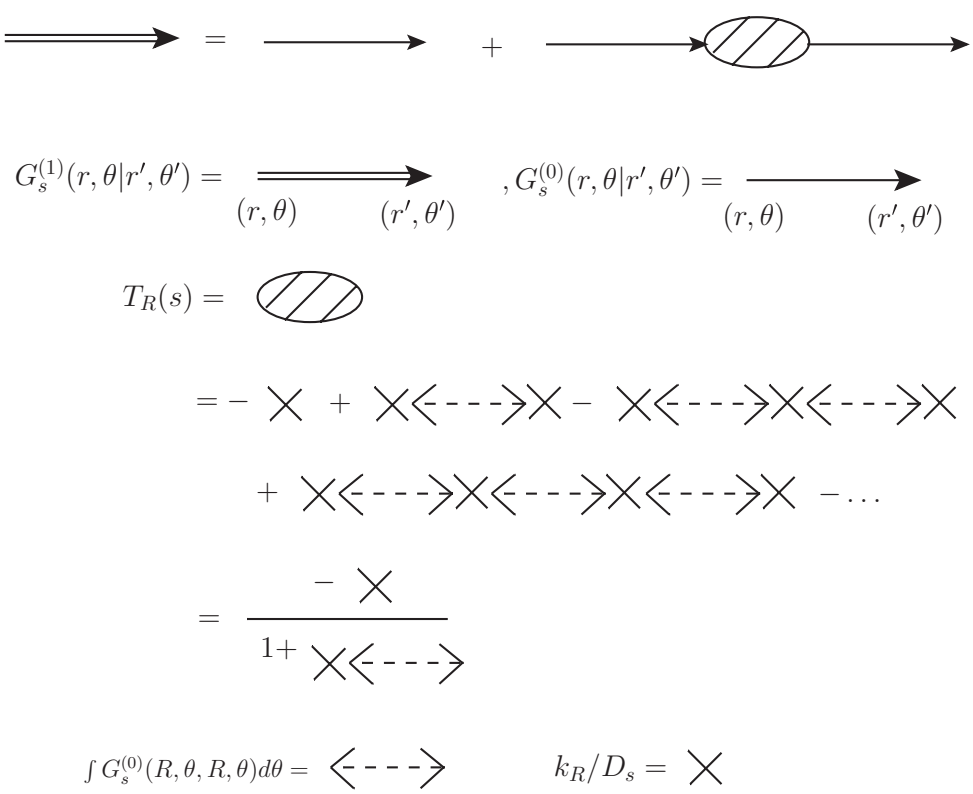

FIG. 10. Green's function $G_s^{(1)}(r,\theta|r',\theta')$ expressed in Feynman diagrams.

Eq. (15) and (16) we find that in the presence of a single ring defect the concentration $S(r)$ and $P(r)$ varies logarithmically as one move away from the ring defect.

V. CONCLUSION

We have presented here a simple model which captures the essential features of reaction-diffusion processes on surfaces having defects. The solution to the problem was obtained by the method of Green's functions. The reaction part of the equation was used as perturbation which was found to be exactly summable. The model describes qualitatively the observed features of pattern formation in Ge clustering on clean Si(111)-(7 × 7) and oxidized Si(111)-(7 × 7) surfaces. First we had shown the formation of patterns in the ring model with four ring defects. The point model was discussed in detail. The time evolution of the reaction diffusion process was explored numerically from the solutions obtained for a case of eight defects distributed uniformly inside the domain. We used further MC simulations to study the point model case for a large number of defects. The first passage time statistics was also studied and obtained empirically the first passage time probability density. These models presented here are real time analysis of the deposition-diffusion-reaction process. It would be very interesting if a thorough time analysis of the formation of patterns is carried out experimentally in future. Finally we note that in this model the product P describes n-mers, $n = 2, 3, \ldots$ we assume that all n-mers have the same diffusion coefficient. However, we believe, this assumption does not seriously affect the result obtained here. In earlier studies on fractal patterns formed in diffusion limited cluster aggregation, the fractal pattern and the fractal dimension were found to be practically the same for the two cases where (i) all clusters have been assumed to have the same diffusion coefficient and (ii) diffusion coefficient was assumed to be inversely proportional to the cluster mass.[30] Definitely, there will be some optimum size of the cluster with

dispersion. So, an improved model must include a sequence of reactions forming clusters. These reactions will also be nonlinear functions of concentration. There will be a dispersion in the diffusion constant of the clusters. Various finer aspects including the effect of geometry of the diffusing surface will be adressed in our future works.

APPENDIX A: DERIVATION OF THE KINETIC EQUATIONS

We denote by S_n a cluster of $n = 2, 3, \ldots, N$ Ge atoms. Various possible one step reactions may occur at a reaction center in which cluster of size n could break to form a cluster of size $n-1$ or an adatom S could coalesce to form a cluster of size $n+1$ (see Fig. 9). The rate equation are given by

$$\frac{dS_n}{dt} = -(k_{-(n-1)} + k_n S)S_n + (k_{n-1} S S_{n-1} + k_n S_{n+1}), \tag{A1}$$

$$\frac{dS_N}{dt} = k_{N-1} S S_{N-1} - k_{-(N-1)} S_N, \tag{A2}$$

where $2 \leq n \leq N-1$.

$$\frac{d}{dt}\sum_{n=2}^{N} S_n = (k_1 S)S - k_{-1} S_2. \tag{A3}$$

We now make the following assumptions (i) All clusters, S_2 to S_N have comparable diffusion coefficients. So, in the first approximation, these can be taken equal. (ii) If $P = \sum_{n=2}^{N} S_n$, we assume that formation of larger clusters at the reaction centers is a very slow process and P is dominated by S_2. So, we replace S_2 by $\sum_{n=2}^{N} S_n$. This need arises for two conciderations. Firstly we have no knowledge of N, though it will not be very large. Secondly, since we want a minimal model which is able to capture the basic physics, we make this approximation to close the equation. So, the assumption is made that the clusters are predominantly of two Ge-atoms. (iii) Even though the formation process is a second order rate process in S, we replace $k_1 S$ by k_f which we call intrinsic clusterization rate of each available reaction center. The rate k_{-1} is redefined as k_b.

Albeit the assumptions incorporated in our model for cluster formation on Si surfaces, appears too simplistic, we are strongly of the opinion that inclusion of all the processes in the clusterization will not significantly change the overall result. On the other hand as we are solving this problem numerically, inclusion of all possible processes of clusterization will increase the time and cost significantly without gaining much in physics. We consider in a separate analysis a reaction scheme in which the cluster formation is second order in substrate S.

APPENDIX B: GREEN'S FUNCTIONS

The Green's function appearing in Eq. (3) are given by

$$G_s^{(1)}(r, \theta | r', \theta') = \sum_{n=0}^{\infty} \left(g_n(r|r') - \frac{g_n(r|R) g_n(R|r')}{g_n(R|R)} \right) \cos(n(\theta - \theta')),$$

$$G_p^{(0)}(r, \theta | r', \theta') = \sum_{n=0}^{\infty} h_n(r|r') \cos(n(\theta - \theta')), \tag{B1}$$

$$\text{where} \quad g_n(r|r') = \begin{cases} \epsilon_n I_n(\sqrt{s/D_s} r) K_n(\sqrt{s/D_s} r') & \text{if} \quad r \leq r', \\ \epsilon_n I_n(\sqrt{s/D_s} r') K_n(\sqrt{s/D_s} r) & \text{if} \quad r > r'. \end{cases} \tag{B2}$$

$$h_n(r|r') = \begin{cases} \epsilon_n I_n(\sqrt{s/D_p}r) K_n(\sqrt{s/D_p}r') & \text{if} \quad r \le r', \\ \epsilon_n I_n(\sqrt{s/D_p}r') K_n(\sqrt{s/D_p}r) & \text{if} \quad r > r'. \end{cases} \tag{B3}$$

with $\epsilon_0 = 1$ and $\epsilon_n = 2$ for all $n = 1, 2. \ldots$

[1] K. Brunner, Rep. Prog. Phys. **65**, 27 (2002); D. Y. Petrovykh, F. J. Himpsel, in: H. S. Nalwa (Ed.), Encyclopedia of Nanoscience and Nanotechnology **9**, 497–528 (2004); B. Voigtlander, M. Kawamura, N. Paul, and V. Cherepanov, J. Phys.: Cond. Mat. **16**, 31535 (2004).
[2] A. Sgarlata, P. D. Szkutnik, A. Balzarotti, N. Motta, and F. Rosei, Appl. Phys. Lett. **83**, 4002 (2003).
[3] H. Omi and T. Ogino, Thin Solid Films **369**, 88 (2000).
[4] T. Ogino, H. Hibino, Y. Homma, Y. Kobayashi, K. Prabhakaran, K. Sumitomo, and H. Omi, Acc. Chem. Res. **32**, 447 (1999).
[5] H. J. Kim, Z. M. Zhao, and Y. H. Xie, Phys. Rev. B **68**, 205312 (2003).
[6] Y. H. Xie, S. B. Samavedam, M. Bulsara, T. A. Langdo, and E. A. Fitzgerald, Appl. Phys. Lett. **71**, 3567 (1997).
[7] H. J. Kim, J. Y. Chang, and Y. H. Xie, J. Cryst. Growth **247**, 251 (2003).
[8] A. K. Das, J. Kamila, B. N. Dev, B. Sundaravel, and G. Kuri, Appl. Phys. Lett. **77**, 951 (2000).
[9] Th. Schmidt, J. I. Flege, S. Gangopadhyay, T. Clausen, A. Locatelli, S. Heun, and J. Falta, Phys. Rev. Lett. **98**, 066104 (2007).
[10] Th. Schmidt, S. Gangopadhyay, J. I. Flege, T. Clausen, A. Locatelli, S. Heun, and J. Falta, New J. Phys. **7**, 193 (2005).
[11] A. Roy, T. Bagarti, K. Bhattacharjee, K. Kundu, and B. N. Dev, Surf. Sci. **606**, 777 (2012).
[12] S. Havlin and D. ben-Avraham, Adv. Phys. **36**, 695 (1987).
[13] H. Taitelbaum and Z. Koza, Physica A **285**, 166 (2000).
[14] P. K. Datta and A. M. Jayannavar, Pramana-J. Phys. **38**, 257 (1992).
[15] P. Grassberger and I. Procaccia, J. Chem. Phys. **77**, 6281 (1982).
[16] Th. M. Nieuwenhuizen and H. Brand, J. Stat. Phys. **59**, 53 (1990).
[17] G. Abramson and H. S. Wio, Chaos Soliton and Fract. **6**, 1 (1995).
[18] C. Mandache and D. ben-Avraham, J. Chem. Phys. **112**, 7735 (2000).
[19] H. Taitelbaum, R. Kopelman, G. H. Weiss and S. Havlin, Phys. Rev. A **41**, 3116 (1990).
[20] R. Kopelman, J. Stat. Phys **42**, 185 (1986).
[21] J. C. Rasaiah, J. B. Hubbard, R. J. Rubin, and S. H. Lee, J. Phys. Chem. **94**, 652 (1990).
[22] A. R. Missel and Karin. A. Dahem, Phys. Rev. E **79**, 021126 (2009).
[23] M. O. Vald, D. H. Rothman, and J. Ross, Physica D **239**, 739 (2010).
[24] Trilochan Bagarti, Anupam Roy, Kalyan Kundu, and B. N. Dev, *Proceeding of Third National Conference on Mathematical Techniques: Emerging Paradigms for Electronics and IT Industries*, University of Delhi, New Delhi (Jan 30-31, 2010) pp. ts-2.1.1–ts-2.1.4.
[25] E. N. Economou, *Green's Functions in Quantum Physics*, third ed., (Springer, Berlin Heidelberg, 2006).
[26] H. S. Carslaw and J. C. Jaeger, *Conduction of Heat in Solids*, second ed., (Oxford University Press, New York, 1959).
[27] J. Abate and P. P. Valko, Int. J. Numerical Meth. Engng. **60**, 979 (2004).
[28] M. Abramowitz and I. A. Stegun, *Handbook of Mathematical Functions*, (Dover Publications Inc., New York, 1972).
[29] S. S. Andrews and D. Bray, Phys. Biol. **1**, 137 (2004).
[30] P. Meakin, Phys. Rev. Lett. **51**, 1119 (1983).